RSC Advances

PAPER

View Article Online
View Journal | View Issue

Cite this: *RSC Adv.*, 2019, **9**, 6762

Structural evolution of LiN_n^+ (n = 2, 4, 6, 8, and 10) clusters: mass spectrometry and theoretical calculations†

Zhongxue Ge,*[ab] Kewei Ding,[ab] Yisu Li,[c] Hongguang Xu,[d] Zhaoqiang Chen,[c] Yiding Ma,[b] Taoqi Li,[b] Weiliang Zhu*[c] and Weijun Zheng*[d]

Received 17th January 2019
Accepted 18th February 2019

DOI: 10.1039/c9ra00439d

rsc.li/rsc-advances

Mixed nitrogen-lithium cluster cations LiN_n^+ were generated by laser vaporization and analyzed by time-of-flight mass spectrometry. It is found that LiN_8^+ has the highest ion abundance among the LiN_n^+ ions in the mass spectrum. Density functional calculations were conducted to search for the stable structures of the Li–N clusters. The theoretical results show that the most stable isomers of LiN_n^+ clusters are in the form of $Li^+(N_2)_{n/2}$, and the order of their calculated binding energies is consistent with that of Li–N_2 bond lengths. The most stable structures of LiN_n^+ evolve from one-dimensional linear type ($C_{\infty v}$, n = 2; $D_{\infty h}$, n = 4), to two-dimensional branch type (D_{3h}, n = 6), then to three-dimensional tetrahedral (T_d, n = 8) and square pyramid (C_{4v}, n = 10) types. Further natural bond orbital analyses show that electrons are transferred from the lone pair on N_α of every N_2 unit to the empty orbitals of lithium atom in LiN_{2-8}^+, while in LiN_{10}^+, electrons are transferred from the bonding orbital of the Li–N_α bonds to the antibonding orbital of the other Li–N_α bonds. In both cases, the N_2 units become dipoles and strongly interact with Li^+. The average second-order perturbation stabilization energy for LiN_8^+ is the highest among the observed LiN_n^+ clusters. For neutral LiN_{2-8} clusters, the most stable isomers were also formed by a Li atom and n/2 number of N_2 units, while that of LiN_{10} is in the form of $Li^+(N_2)_3(\eta^1\text{-}N_4)$.

1 Introduction

Nitrogen clusters have been predicted to be potential high energy density materials (HEDM)[1,2] by numerous theoretical[3,4] studies. Since the identification of N_5^+, N_4, and N_5^-,[5–7] the search for new polynitrogen species by a variety of experimental techniques has received intense attention. However, only a few efforts have been successful due to the low stability of these clusters. Metal doped nitrogen clusters MN_n have advantages in designing new polynitrogen structural groups because the metal–nitrogen interactions may be able to stabilize polynitrogen groups in MN_n with respect to the corresponding isolated N_n species.[8] Many novel polynitrogen structural groups such as cyclic N_4,[9–12] N_5,[13] N_6,[14] and N_7 (ref. 15) have been predicted to exist in this form. Thus, it is interesting to generate metal-doped nitrogen clusters, gradually increase their nitrogen content and study their structural characteristics.

To date, extensive experimental works have been undertaken to investigate mixed nitrogen–metal clusters. Numerous homoleptic azides of the type $M(N_3)_n$ (M = Ti, Nb, Ta, Mo, W, *etc.*)[16–27] and their derived salts have been prepared and characterized to understand the properties of highly energetic materials. $Nb^+(N_2)_n$ and $V^+(N_2)_n$ complexes were investigated using photodissociation spectroscopy.[28,29] $Rh(N_2)_4^+$ complexes were studied by infrared laser photodissociation spectroscopy and theoretical calculations.[30] TiN_{12}^+ was generated by laser ablation, and the most stable structure was found to be $Ti(N_2)_6^+$ with O_h symmetry.[31] The VN_n^+ (n = 8, 9, and 10) clusters were generated and their most stable isomers were found to be in the form of $V(N_2)_4^+$, $(\eta^2\text{-}N_4)V^+N(N_2)_2$ and $(\eta^4\text{-}N_4)V^+(N_2)_3$, respectively.[32]

Lithium is the lightest metal. It is highly reactive and can react with nitrogen gas to form lithium nitride.[33] In addition, lithium atoms have been successfully used as dopants in many clusters, such as silicon,[34] germanium,[35] boron[36] and aluminum[37] clusters, to tailor their structural and electronic properties. Although the experimental studies on lithium-doped nitrogen clusters were very scarce, these clusters have been investigated in preliminary studies by many theoretical calculations. Cheng and Li predicted that lithium and N_4^{2-} ring could form bipyramidal Li_2N_4 structures[38] with significant barriers for isomerization and dissociation. Glukhovtsev and

[a]State Key Laboratory of Fluorine & Nitrogen Chemicals, Xi'an 710065, China
[b]Xi'an Modern Chemistry Research Institute, Xi'an 710065, China. E-mail: gzx204@sina.com.cn
[c]Drug Discovery and Design Center, Shanghai Institute of Materia Medica, Chinese Academy of Sciences, Shanghai 201203, China. E-mail: wlzhu@mail.shcnc.ac.cn
[d]Beijing National Laboratory for Molecular Sciences (BNLMS), State Key Laboratory of Molecular Reaction Dynamics, Institute of Chemistry, Chinese Academy of Sciences, Beijing 100190, China. E-mail: zhengwj@iccas.ac.cn

† Electronic supplementary information (ESI) available: Similar mass spectra and NBO data of the Li–N clusters. See DOI: 10.1039/c9ra00439d

Schleyer studied the structure and stability of N_5Li and found that N_5Li favours a planar C_{2v} structure.[39] Investigation of lithium–nitrogen clusters may provide useful information for understanding the lithium–nitrogen interactions and for the design of high nitrogen content species.

In this work, we investigated lithium–nitrogen binary clusters by laser ablation experiments coupled with theoretical calculations to gain insights into the geometric structures and electronic properties of LiN_n^+ and their neutral counterparts.

2 Experimental and theoretical methods

2.1 Experimental method

The experiments were conducted using a home-built apparatus equipped with a laser vaporization supersonic cluster source and a reflectron time-of-flight mass spectrometer (RTOF-MS) that has been described elsewhere.[40] The laser vaporization source was cooled by liquid nitrogen. The disk targets made of LiCl, LiF, LiF/ZrN (mole ratio 4 : 1), LiF/AlN (mole ratio 2 : 1) or LiF/BN (mole ratio 2 : 1) were used in the experiments to provide Li^+ ions. The LiN_n^+ ($n = 2$, 4, 6, 8, and 10) cluster cations were generated in the laser vaporization source by laser ablation the rotating and translating disk targets in N_2 gas with the second harmonic of a nanosecond Nd:YAG laser (Continuum Surelite II-10). Nitrogen carrier gas with ~4 atm backing pressure was allowed to expand through a pulsed valve (General Valve Series 9) into the source to provide nitrogen and to cool the formed clusters. The typical laser power used in this work was approximately 10 mJ per pulse. The generated cluster cations were mass-analysed by the RTOF-MS.

2.2 Theoretical methods

The geometry optimization and frequency calculations were performed with Gaussian 09 program package using density functional theory (DFT) at the M06-2X/6-311+G(d,p) level.[41–43] Every stationary point on the potential energy surface (PES) was confirmed to be local minimum-energy structure by all positive harmonic frequencies. The bond length of the N_2 molecule was calculated to verify the accuracy of the theoretical method. The calculated N–N bond length is about 1.090 Å, which is consistent with an experimental value of 1.097 Å.[44] The binding energies of nitrogen to $Li^{+/0}$ were calculated for each $LiN_n^{+/0}$ species. The binding energy is defined as:

$$E_{b1} = 2[E(Li) + n/2E(N_2) - E(LiN_n)]/n \text{ (for the neutrals)} \quad (I)$$

$$E_{b2} = 2[E(Li^+) + n/2E(N_2) - E(LiN_n^+)]/n \text{ (for the cations)}$$

To get further insight into the interactions between N_2 molecule and $Li^{+/0}$, we performed natural bond orbital (NBO) analysis[45] where the electronic wave function is interpreted in terms of a set of occupied Lewis orbitals and a set of unoccupied non-Lewis delocalized orbitals. For each donor NBO (i) and acceptor NBO (j), the stabilization energy E_2 associated with charge transfer $i \rightarrow j$ is given by

$$E(2) = \Delta E_{ij} = q_i F(i,j)^2/(\varepsilon_i - \varepsilon_j) \quad (II)$$

where q_i is the donor orbital occupancy, and ε_i and ε_j are diagonal elements (orbital energies) and $F(i,j)$ is the off-diagonal NBO Fock matrix element.

The average $E(2)$ of LiN_n^+ is defined as:

$$\overline{E(2)} = 2\left[\sum E(2)\right]\Big/n \quad (III)$$

3 Experimental results

Fig. 1 shows a typical mass spectrum of the clusters generated in the experiment with LiCl as the substrate and N_2 as the carrier gas. It is observed that the main series of lithium–nitrogen clusters are LiN_2^+, LiN_4^+, LiN_6^+, LiN_8^+ and LiN_{10}^+. The mass intensity of LiN_8^+ is predominant compared to those of the other LiN_n^+ species. No mass peak of LiN_n^+ with odd numbers of nitrogen atoms has been detected. In addition to the mass peaks of lithium–nitrogen clusters, the mass peaks of $LiN_2(H_2O)^+$, $LiN_4(H_2O)^+$, $LiN_6(H_2O)^+$ and $LiN_8(H_2O)^+$ are also observed. The formation of $LiN_n(H_2O)^+$ more likely is due to the presence of trace amounts of water in the carrier gas. In laser ablation experiments with LiF, LiF/ZrN, LiF/AlN and LiF/BN as substrates, similar lithium–nitrogen clusters were obtained (ESI, Fig. S1–S4†).

4 Theoretical results

To search for the stable structures of LiN_n^+ and LiN_n ($n = 2$, 4, 6, 8, and 10), we have conducted calculations for nine different categories of structures, from LiN_2 to LiN_{10}. Starting from the simplest one containing only two nitrogen atoms and a lithium atom, by adding one nitrogen atom at a time to the system, we obtained an increasing number of geometrical configurations as the system

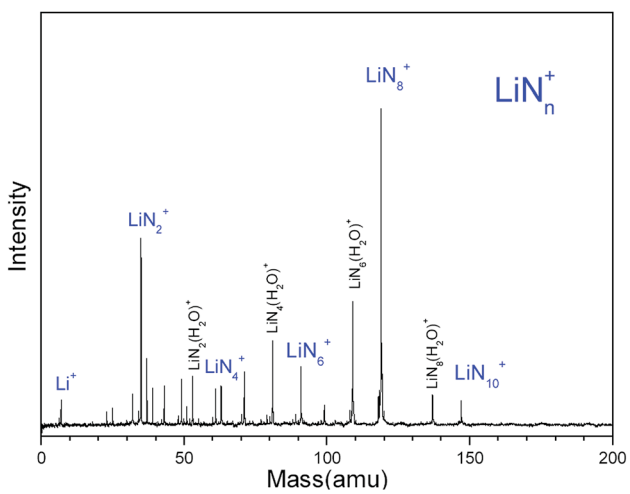

Fig. 1 Typical mass spectrum of Li–N clusters generated by laser ablation of a LiCl target with N_2 as the carrier gas.

became larger. By placing the nitrogen atoms at different locations, we constructed the initial geometrical structures with a series of units such as N_2 molecules, N_3 chain and ring, N_4 chain and ring, and N_5, N_6, and N_7 rings and so on containing lithium atoms. To ensure that the geometry optimizations located the true minima on the potential surfaces, frequency calculations were conducted for all optimized structures. For each initial geometrical configuration, we also considered many spin multiplicities (2, 4, and 6 for neutral species and 1, 3, and 5 for positive ions). After full relaxation, a rather large number of low-lying isomers of LiN_n^+ and LiN_n (n = 2, 4, 6, 8, and 10) were found. Here, we show the typical isomers of LiN_n^+ (n = 2, 4, 6, 8, and 10) in Fig. 2 with the most stable structures on the left and those of LiN_n (n = 2, 4, 6, 8, and 10) in Fig. 3.

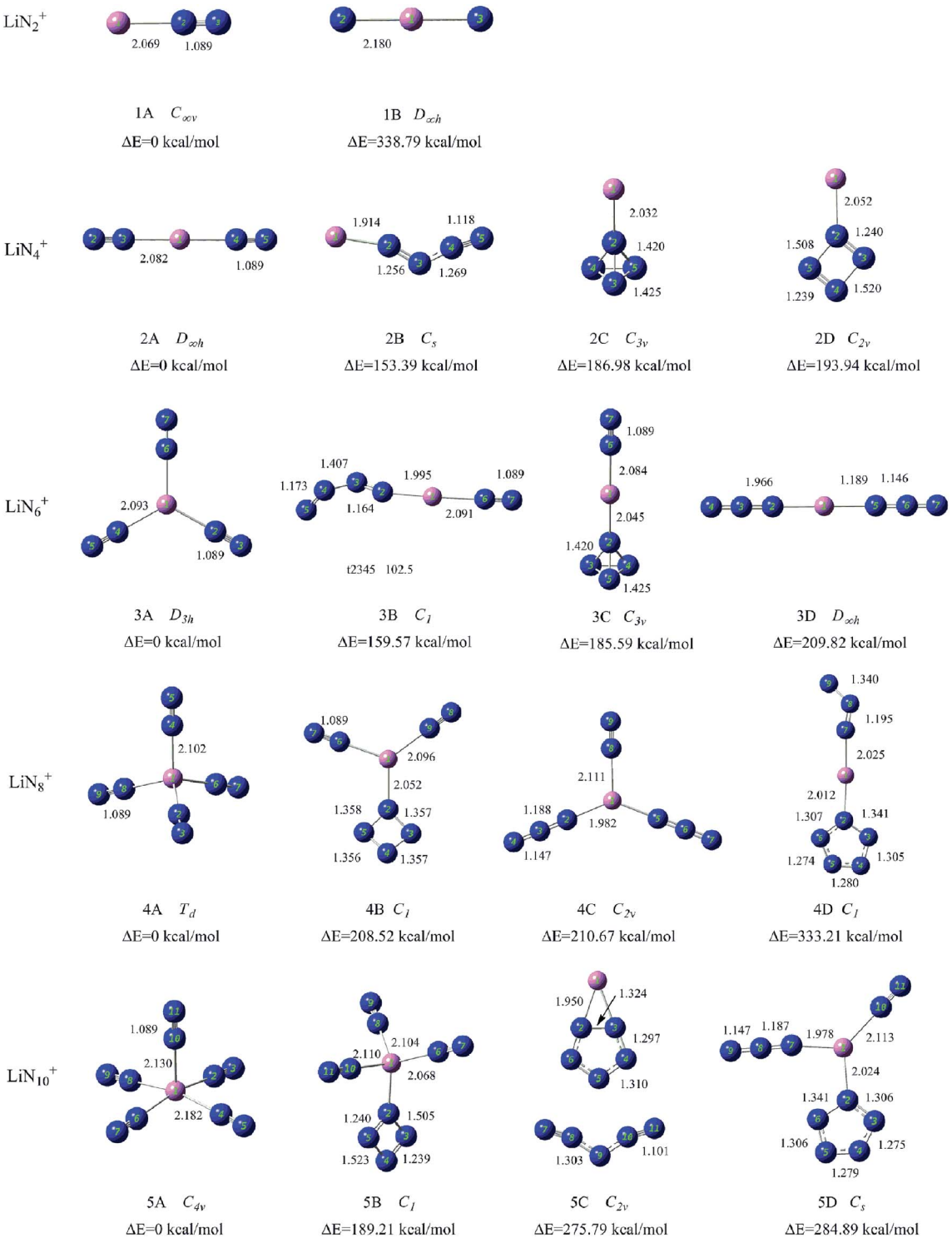

Fig. 2 Typical low-lying isomers of LiN_n^+ (n = 2, 4, 6, 8, and 10) clusters. The bond lengths are given in angstroms.

4.1 Structures of LiN_2^+ and LiN_2

The ground state structure of LiN_2^+ (1A) is a $C_{\infty v}$ symmetry linear structure formed by attaching an end-on N_2 molecule to a Li atom. The N–N bond lengths in the N_2 unit are 1.089 Å. The second isomer (1B) is a $D_{\infty h}$ symmetry linear structure formed by inserting a Li atom between two N atoms. It is much higher in energy than 1A.

For neutral LiN_2, the most stable isomer 1A′ has a C_{2v} symmetry triangular structure consisting of a side-on N_2 molecule and an Li atom. The N–N bond length in the side-on N_2 unit is 1.168 Å, which is longer than that of isolated N_2 molecule. The second stable structure 1B′ has one end-on N_2 unit and one Li atom, similar to 1A of LiN_2^+. However, the N–N bond length in the end-on N_2 unit increases to 1.386 Å.

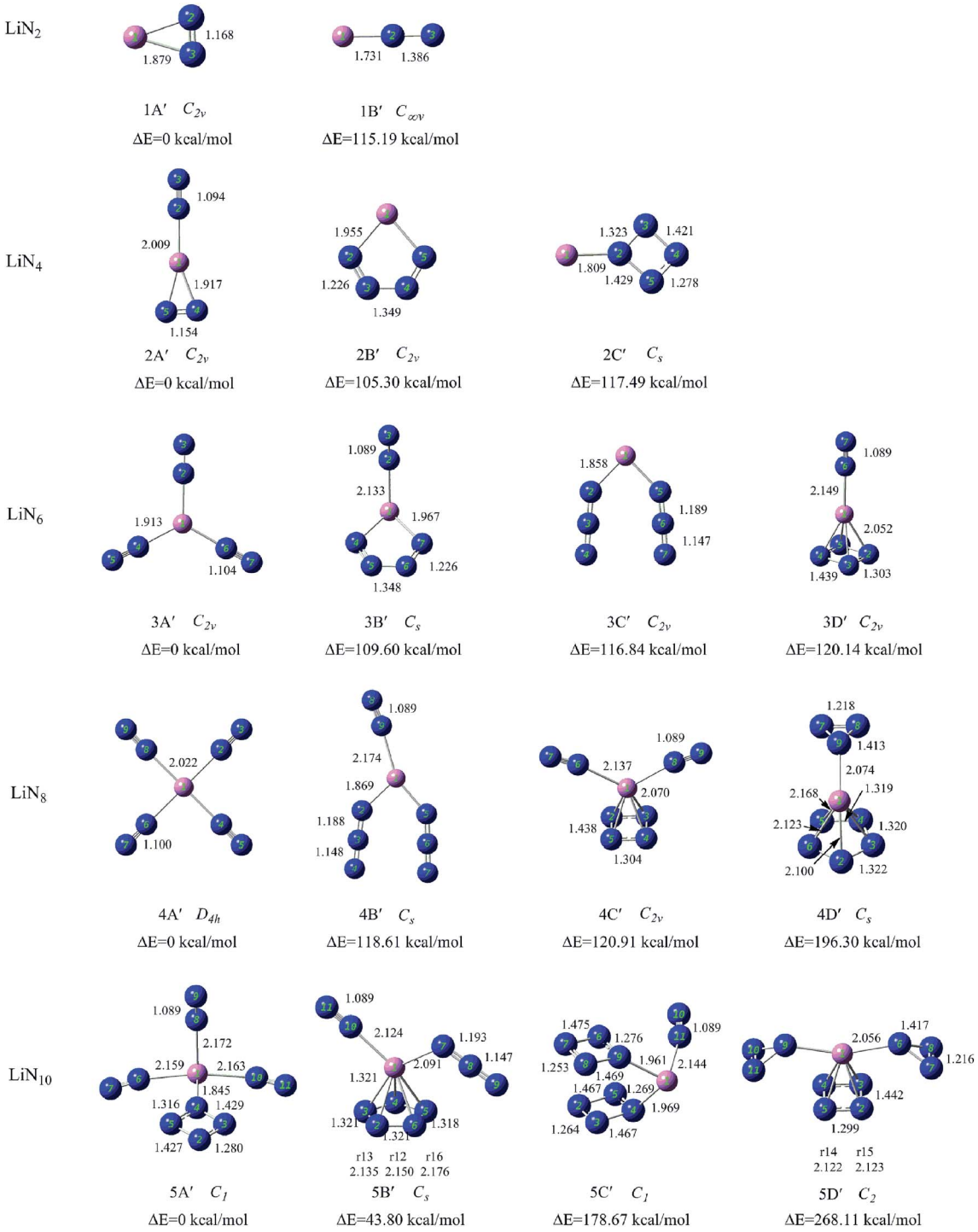

Fig. 3 Structures and relative energies of the low-lying isomers of neutral LiN_n (n = 2, 4, 6, 8, and 10) clusters. The bond lengths are given in angstroms.

4.2 Structures of LiN_4^+ and LiN_4

The ground state structure of LiN_4^+ (2A) is a $D_{\infty h}$ symmetry linear structure, in which two N_2 molecules are attached directly to the central Li atom. The N–N bond lengths in the N_2 units are 1.089 Å. In the other low-lying isomers of LiN_4^+ (2B–2D), N_4 units were found and they interact with Li atoms as a whole. For example, in isomers 2B, 2C and 2D, the N_4 units exhibit chain, tetrahedral, and cyclic configurations, respectively, and connect to Li atom *via* one nitrogen atom. These N_4 units have been reported in many previous studies and the interaction between Li^+ and N_4 ring was also predicted by Li *et al.*[38,46–48]

For neutral LiN_4, isomer 2A′ with one end-on and one side-on distances of the end-on and side-on N_2 units are 1.094 and 1.154 Å, respectively. A N_4 chain is found in isomer 2B′ and is connected to the Li atom through two terminal nitrogen atoms. Isomer 2C′ has a Li atom interacting with a η^1-N_4 ring similar to isomer 2D LiN_4^+. We could not find any isomer with a tetrahedral $N_4(T_d)$ unit in neutral LiN_4.

4.3 Structures of LiN_6^+ and LiN_6

For LiN_6^+, the lowest energy isomer (3A) has a planar structure with D_{3h} symmetry, in which three N_2 molecules interact equally with the central Li atom *via* their terminal nitrogen atoms. The N–N bond lengths in the N_2 units are 1.089 Å. The low-lying isomers containing other all-nitrogen units are also found and their energies are much higher than that of 3A. Isomer 3B has one end-on bound N_2 molecule and one N_4 chain coordinating to the Li atom *via* their terminal nitrogen atoms. The N_4 chain can be regarded as a complex of two N_2 sub-units because the bond linking the two N_2 sub-units is relatively weak. Isomer 3C contains one end-on bound N_2 molecule and one tetrahedral N_4 unit that coordinates to the Li atom through one vertex nitrogen atom. Isomer 3D is a $D_{\infty h}$ symmetry linear structure formed by attaching two N_3 ligands to the Li atom.

The ground state structure of LiN_6 (3A′) is similar to that of LiN_6^+ (3A). It was also formed by attaching three N_2 molecules to the central Li atom, but its symmetry changes to C_{2v}. In the other low-lying isomers, N_3, N_4 and N_6 units are the main building blocks. Isomer 3B′ contains one end-on bound N_2 molecule and one N_4 chain that connects to the Li atom through its two terminal nitrogen atoms. Isomer 3C′ has two end-on N_3 units. Isomer 3D′ has one end-on N_2 molecule and one η^4-N_4 ring.

4.4 Structures of LiN_8^+ and LiN_8

The most stable structure of LiN_8^+ (4A) is a T_d symmetry structure formed by attaching four end-on N_2 molecules to a Li atom. The N–N bond lengths in the N_2 units are 1.089 Å. The other low-lying isomers are much higher in energy than 4A. Isomer 4B has one η^1-N_4 ring and two end-on bound N_2 molecules. Isomer 4C contains two N_3 units and one end-on bound N_2 molecule. 4D has one η^1-N_5 ring and one N_3 unit. The planar structure Li-η^1-N_5 in 4D was also studied by Glukhovtsev and considered as a possible isomer of LiN_5.[39]

For LiN_8, the lowest energy isomer (4A′) has a planar structure with D_{4h} symmetry in which four N_2 molecules interact equally with the central Li atom *via* their terminal nitrogen atoms. The N–N bond lengths in the N_2 units are 1.089 Å. Isomer 4B′ was formed by attaching two N_3 units and one end-on bound N_2 molecule to a Li atom. Isomer 4C′ has one η^4-N_4 ring and two end-on bound N_2 molecules. Isomers 4B′ and 4C′ could be considered to evolve from isomers 3C′ and 3D′ by the addition of one end-on bound N_2 molecule. Isomer 4D′ has one η^5-N_5 ring and one η^1-N_3 units. This pyramidal structure formed by N_5 ring and metal ions has been proposed in many theoretical studies.[39,49,50] $[N_3MN_5]^q$ structure was also calculated by Jin *et al.*, and their results suggested that the $[N_3MN_5]^q$ in heterodecked form are thermodynamically more stable than the sandwich-like isomers $[N_4MN_4]^q(D_{4d})$ with even-membered N_4^{2-} ring [(M, q) = (Ni, 0), (Co, −1), (Fe, −2)].[51]

4.5 Structures of LiN_{10}^+ and LiN_{10}

The most stable isomer of LiN_{10}^+ (5A) consists of five N_2 molecules placed around the Li atom and exhibits C_{4v} symmetry. 5B is the second stable structure and has three N_2 molecules and one η^1-N_4 ring and its energy is much higher than that of 5A. The third isomer 5C has one N_{10} unit consisting of an N_5 ring and an N_5 chain. This N_{10} unit was similar to the $N_5^+N_5^-$ ionic compound.[52] Isomer 5D is the fourth stable structure and has one η^1-N_5 ring, one N_2 and one N_3 unit.

The low-lying isomers of neutral LiN_{10} are different from those of its positive charged counterpart. As shown in Fig. 3, 5A′ has three N_2 molecules and one η^1-N_4 ring. 5B′ consists of one N_2 molecule, one N_3 unit and one η^5-N_5 ring. It is higher in energy than 5A′ by 43.80 kcal mol^{-1}. Isomer 5C′ consists of two face-to-face η^1-N_4 rings and one N_2 unit. The adjacent N_4 rings anchored on the Li atom in 5C′ are a precursor for the formation of other all-nitrogen structures. The most stable isomer with the N_3 ring is 5D′ that has two η^1-N_3 rings and one η^4-N_4 ring. The nitrogen rings in 5D′ make it a highly energetic cluster.

5 Discussion

5.1 Structure of Li–N clusters

In our experiments, it is found that LiN_n^+ clusters (n = 2, 4, 6, 8, and 10) can be generated by laser ablation of LiCl without any solid nitrogen source, indicating that the carrier gas (N_2) used in the experiments participated in the formation of Li–N clusters. The LiN_n^+ clusters generated in our experiment all have even numbers of nitrogen atoms, suggesting that the generated LiN_n^+ clusters may be formed by N_2 sub-units.

As shown in Fig. 3, the most stable isomers of LiN_n^+ (1A–5A) obtained by theoretical calculations are formed by a lithium cation and a number of end-on bound N_2 units, that is in the form of $Li^+(N_2)_{n/2}$. This is consistent with the facts that the generated LiN_n^+ cluster cations all have even number of nitrogen atoms and their numbers of nitrogen atoms differ by multiples of 2. An examination of the most stable isomers 1A–5A shows that the structures of these observed LiN_n^+ (n = 2, 4, 6, 8, and 10) cluster cations evolve from one-dimensional linear type ($C_{\infty v}$, $D_{\infty h}$) to two-dimensional branch type (D_{3h}) to three-dimensional tetrahedral (T_d) and square pyramid (C_{4v}) types

Table 1 Binding energies and Li–N_2 distances of the most stable isomers of $LiN_n^{+/0}$ (n = 2, 4, 6, 8, and 10)

Positive cluster		Symmetry	Multiplicity	Li–N_2 distance	E_b (eV)	Neutral cluster		Symmetry	Multiplicity	Li–N_2 distance	E_b (eV)
Li–N_2^+	1A	$C_{\infty v}$	1	2.069	0.57	Li–N_2	1A′	C_{2v}	2	1.879	−0.12
Li–N_4^+	2A	$D_{\infty h}$	1	2.082	0.54	Li–N_4	2A′	C_{2v}	2	2.009, 1.917	0.12
Li–N_6^+	3A	D_{3h}	1	2.093	0.51	Li–N_6	3A′	C_{2v}	2	1.913	0.23
Li–N_8^+	4A	T_d	1	2.102	0.49	Li–N_8	4A′	D_{4h}	2	2.022	0.26
Li–N_{10}^+	5A	C_{4v}	1	2.172[a]	0.45	Li–N_{10}	5A′	C_1	2	2.165[a]	−0.79

[a] The average Li–N_2 distance.

with increasing number of N_2 units. LiN_8^+ has a highly symmetrical structure with T_d symmetry. It also has high nitrogen content (94.1%) and may be used as a potential precursor for production of poly-nitrogen species.

Among the low-lying isomers of $LiN_n^{+/0}$ (n = 2, 4, 6, 8, and 10) presented in Fig. 2 and 3, the end-on bound N_2 units are the most common with the N–N bond lengths of approximately 1.09 Å, which are nearly the same as those in isolated nitrogen molecules. The side-on bound N_2 units are found in isomers 1A′ and 2A′, and the N–N bonds in these clusters are clearly weakened by coordination and the N–N bond lengths increase to approximately 1.16 Å. In addition, the isomers with a high number of N_2 units commonly have relatively lower energies than those with the other all-nitrogen units. This is very similar to the results obtained in our previous studies.[31,32]

Other all-nitrogen groups, such as linear N_3, circular N_3, chain-shaped N_4, circular N_4, tetrahedral N_4, circular N_5, circular N_6 and so on, were also found in the low-lying isomers of $LiN_n^{+/0}$ (n = 2, 4, 6, 8, and 10) clusters. This suggests that the doping of lithium atom could promote the stability of the above all-nitrogen groups, and these energetic $LiN_n^{+/0}$ (n = 2, 4, 6, 8, and 10) isomers may exist in principle. Many N_5 units found in $LiN_n^{+/0}$ isomers were in the form of the η^1-N_5 ring, which is consistent with the coordination mode of compounds synthesized to date such as $[M(H_2O)_4(N_5)_2]\cdot 4H_2O$ (M = Mn, Fe and Co).[53,54]

5.2 Binding energies of the most stable isomers

To estimate the strength of the interactions between the Li atom and nitrogen ligands, we calculated the binding energies of the most stable isomers of $LiN_n^{+/0}$ (n = 2, 4, 6, 8, and 10). The calculation results are shown in Table 1 and Fig. 4. The Li–N_2 distances in $LiN_n^{+/0}$ (n = 2, 4, 6, 8, and 10) are also listed in Table 1 for comparison.

An examination of the results presented in Table 1 and Fig. 4 shows that binding energies of the ground states of LiN_n^+ (n = 2, 4, 6, 8, and 10) are positive, suggesting a substantial energy stabilization of the LiN_n^+ (n = 2, 4, 6, 8, and 10) species compared to the bare Li cation and N_2 molecules. The stabilizing effects decrease slowly as the numbers of end-on bound N_2 units increase. Considering that the N–N distances in the N_2 units of LiN_n^+ (n = 2, 4, 6, 8, and 10) are all equal to that of the N_2 molecules calculated in this work, we wish to stress that the calculated binding energies reflect the Li–N_2 bond strengths in the clusters. Moreover, as shown in Table 1, the Li–N_2 distances were found to be in the order of $LiN_2^+ < LiN_4^+ < LiN_6^+ < LiN_8^+ < LiN_{10}^+$, which is consistent with the order of the binding energies.

For neutral LiN_n (n = 2, 4, 6, 8, and 10) clusters, with the exception of the 1A′ and 5A′ clusters, the binding energies of the ground states are also positive, indicating the presence of similar stabilizing effects. However, for 1A′ with only one side-on bound N_2 unit, the binding energy is negative, possibly because the side-on bound N_2 unit has a higher energy than the N_2 molecule due to the weakening of the N–N bond (1.168 Å). The binding energy of 5A′ with N_4 rings is also negative and is much lower than those of the other stable Li–N isomers. This is because the energetic N_4 ring drastically increases the relative energy of isomer 5A′.

5.3 NBO analyses for the most stable isomers of LiN_n^+

To further understand the binding and electronic structures of the Li–N clusters observed in the mass spectra, we performed NBO analyses for the most stable isomers of LiN_n^+ (n = 2, 4, 6, 8, and 10), and the calculated results are presented in Tables S1–S5.† In the NBO model, the strength of the interaction of the electron donor and electron acceptor NBOs is defined by the stabilization energy $E(2)$. To evaluate the general contribution of all of the interactions between the electron donors and electron acceptors to the stabilization energy of the LiN_n^+ clusters, the sum of all of the stabilization energies, $\sum E(2)$, was divided by

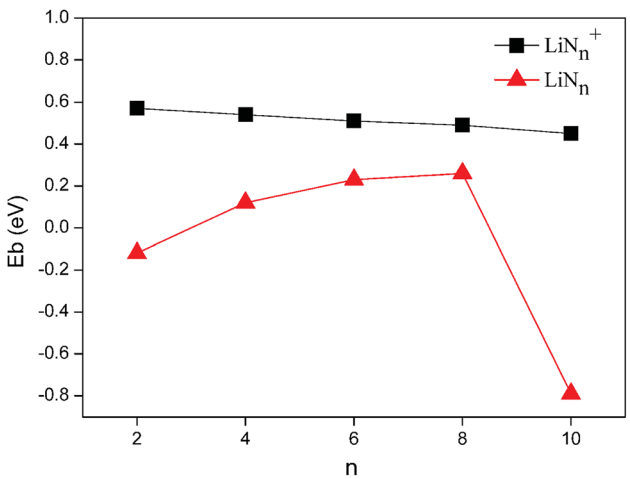

Fig. 4 Binding energies of the most stable isomers of $LiN_n^{+/0}$ (n = 2, 4, 6, 8, and 10) clusters.

Table 2 The NPA charge distributions and second-order perturbation stabilization energies of the most stable isomers of the $Li^+-(N_\alpha{\equiv}N_\beta)_{n/2}$ clusters

Cluster		q (Li)	q (N_α)	q (N_β)	Charge transfer	$\overline{E(2)}$ (kcal mol^{-1})
$Li-N_2^+$	1A	0.97607	−0.19289	0.21682	$LP(1)N_\alpha \rightarrow LP^*Li$	8.93
$Li-N_4^+$	2A	0.89635	−0.15482	0.20665	$LP(1)N_\alpha \rightarrow LP^*Li$	22.65
$Li-N_6^+$	3A	0.76153	−0.11126	0.19075	$LP(1)N_\alpha \rightarrow LP^*Li$	37.36
$Li-N_8^+$	4A	0.59306	−0.07581	0.17754	$LP(1)N_\alpha \rightarrow LP^*Li$	50.48
$Li-N_{10}^+$	5A	0.47380	−0.05275	0.15651	$BD(1)Li-N_\alpha \rightarrow BD^*(1)Li-N_\alpha$	31.32
			−0.05449	0.16567		

the number of N_2 units, as shown in eqn (III), to obtain the average stabilization energy, $\overline{E(2)}$. Table 2 shows the NPA charge distributions and average second-order perturbation stabilization energies of the most stable isomers of the LiN_n^+ clusters.

Based on the NBO data, it was concluded that for LiN_n^+ (n = 2, 4, 6, 8), electrons are transferred from the lone pair (LP) on N_α of every N_2 unit to the empty orbital LP* of the lithium atom, $LP(1)N_\alpha \rightarrow LP^*Li$, leading to a lowering in the average stabilization energy by 8.93, 22.65, 37.36 and 50.48 kcal mol^{-1}, respectively. Meanwhile, for LiN_{10}^+, the interaction is occurs mainly between the Li_1–N_2, Li_1–N_4, Li_1–N_6 and Li_1–N8 bonds, and the electrons are transferred from the bonding orbital (BD) of the Li–N_α bonds to the antibonding orbital (BD*) of the other Li–N_α bonds, giving rise to the $\overline{E(2)}$ values of approximately 31.32 kcal mol^{-1}. In both cases, the N_α and N_β in N_2 units carry negative and positive charges, respectively, forming a dipole that strongly interacts with Li^+. The average stabilization energy, $\overline{E(2)}$, of LiN_8^+ is the highest among the LiN_n^+ (n = 2, 4, 6, 8, and 10) clusters, providing a partial explanation for the highest abundance of LiN_8^+ in the mass spectra.

6 Conclusions

LiN_n^+ (n = 2, 4, 6, 8, and 10) clusters were generated by laser ablation. LiN_8^+ is found to be the most abundant. Density functional calculations were conducted to search for the stable structures of $LiN_n^{+/0}$. The theoretical results show that the most stable isomers of LiN_n^+ (n = 2, 4, 6, 8, and 10) are in the form of $Li^+(N_2)_{n/2}$, and their structures evolve from one-dimensional linear type ($C_{\infty v}$, n = 2; $D_{\infty h}$, n = 4), to two-dimensional branch type (D_{3h}, n = 6) to three-dimensional tetrahedral (T_d, n = 8) and square pyramid (C_{4v}, n = 10) types. The calculated binding energies suggest a substantial energy stabilization of the LiN_n^+ (n = 2, 4, 6, 8, and 10) species compared to the bare Li cation and N_2 molecules. Further NBO analyses show that the N_2 units in LiN_n^+ are actually dipoles that could interact with Li^+ effectively, and LiN_8^+ has the highest average stabilization energy. For neutral LiN_n (n = 2, 4, 6, and 8) clusters, the most stable isomers were also formed by a Li atom and the corresponding number of N_2 units, while the most stable isomer of LiN_{10} is in the form of $Li^+(N_2)_3(\eta^1\text{-}N_4)$.

Conflicts of interest

There are no conflicts to declare.

Acknowledgements

This work was supported by the National Natural Science Foundation of China (Grant No. 21103202 and 21273246).

Notes and references

1 W. J. Lauderdale, J. F. Stanton and R. J. Bartlett, *J. Phys. Chem.*, 1992, **96**, 1173–1178.
2 H. Östmark, *New Trends in Research of Energetic Materials Czech Republic*, 2006, pp. 231–250.
3 P. C. Samartzis and A. M. Wodtke, *Int. Rev. Phys. Chem.*, 2006, **25**, 527–552.
4 M. N. Glukhovtsev, H. Jiao and P. v. R. Schleyer, *Inorg. Chem.*, 1996, **35**, 7124–7133.
5 K. O. Christe, W. W. Wilson, J. A. Sheehy and J. A. Boatz, *Angew. Chem., Int. Ed.*, 1999, **38**, 2004–2009.
6 F. Cacace, G. de Petris and A. Troiani, *Science*, 2002, **295**, 480–481.
7 A. Vij, J. G. Pavlovich, W. W. Wilson, V. Vij and K. O. Christe, *Angew. Chem., Int. Ed.*, 2002, **41**, 3051–3054.
8 L. Gagliardi and P. Pyykkö, *J. Phys. Chem. A*, 2002, **106**, 4690–4694.
9 G. von Zandwijk, R. A. J. Janssen and H. M. Buck, *J. Am. Chem. Soc.*, 1990, **112**, 4155–4164.
10 Q. S. Li and L. P. Cheng, *J. Phys. Chem. A*, 2003, **107**, 2882–2889.
11 L. P. Cheng and Q. S. Li, *J. Phys. Chem. A*, 2005, **109**, 3182–3186.
12 J. M. Mercero, J. M. Matxain and J. M. Ugalde, *Angew. Chem., Int. Ed.*, 2004, **43**, 5485–5488.
13 L. Jin and Y.-h. Ding, *J. Phys. Chem. A*, 2009, **113**, 13645–13650.
14 A. C. Tsipis and A. T. Chaviara, *Inorg. Chem.*, 2004, **43**, 1273–1286.
15 M. Lein, *Chem.–Eur. J.*, 2001, **7**, 4155–4163.
16 R. Haiges, J. A. Boatz, S. Schneider, T. Schroer, M. Yousufuddin and K. O. Christe, *Angew. Chem., Int. Ed.*, 2004, **43**, 3148–3152.
17 R. Haiges, J. A. Boatz, T. Schroer, M. Yousufuddin and K. O. Christe, *Angew. Chem., Int. Ed.*, 2006, **45**, 4830–4835.
18 R. Haiges, J. A. Boatz, M. Yousufuddin and K. O. Christe, *Angew. Chem., Int. Ed.*, 2007, **46**, 2869–2874.
19 R. Haiges, J. A. Boatz and K. O. Christe, *Angew. Chem., Int. Ed.*, 2010, **49**, 8008–8012.

20 R. Haiges, J. A. Boatz, R. Bau, S. Schneider, T. Schroer, M. Yousufuddin and K. O. Christe, *Angew. Chem., Int. Ed.*, 2005, **44**, 1860–1865.
21 A. C. Filippou, P. Portius, D. U. Neumann and K.-D. Wehrstedt, *Angew. Chem., Int. Ed.*, 2000, **39**, 4333–4336.
22 P. Portius, A. C. Filippou, G. Schnakenburg, M. Davis and K.-D. Wehrstedt, *Angew. Chem., Int. Ed.*, 2010, **49**, 8013–8016.
23 A. C. Filippou, P. Portius and G. Schnakenburg, *J. Am. Chem. Soc.*, 2002, **124**, 12396–12397.
24 A. Villinger and A. Schulz, *Angew. Chem., Int. Ed.*, 2010, **49**, 8017–8020.
25 C. Knapp and J. Passmore, *Angew. Chem., Int. Ed.*, 2004, **43**, 4834–4836.
26 T. M. Klapötke, B. Krumm, M. Scherr, R. Haiges and K. O. Christe, *Angew. Chem., Int. Ed.*, 2007, **46**, 8686–8690.
27 T. M. Klapötke, B. Krumm, P. Mayer and I. Schwab, *Angew. Chem., Int. Ed.*, 2003, **42**, 5843–5846.
28 E. D. Pillai, T. D. Jaeger and M. A. Duncan, *J. Am. Chem. Soc.*, 2007, **129**, 2297–2307.
29 E. D. Pillai, T. D. Jaeger and M. A. Duncan, *J. Phys. Chem. A*, 2005, **109**, 3521–3526.
30 A. D. Brathwaite, H. L. Abbott-Lyon and M. A. Duncan, *J. Phys. Chem. A*, 2016, **120**, 7659–7670.
31 K. W. Ding, X. W. Li, H. G. Xu, T. Q. Li, Z. X. Ge, Q. Wang and W. J. Zheng, *Chem. Sci.*, 2015, **6**, 4723–4729.
32 K. W. Ding, H. G. Xu, Y. Yang, T. Q. Li, Z. Q. Chen, Z. X. Ge, W. L. Zhu and W. J. Zheng, *J. Phys. Chem. A*, 2018, **122**, 4687–4695.
33 A. M. Sapse and P. V. R. Schleyer, *Lithium Chemistry: Theoretical and Experimental Overview*, Wiley Interscience, New York, USA, 1995.
34 D. Hao, J. Liu and J. Yang, *J. Phys. Chem. A*, 2008, **112**, 10113–10119.
35 T. B. Tai and M. T. Nguyen, *Chem. Phys. Lett.*, 2010, **492**, 290–296.
36 L. F. Gong, W. L. Guo, X. M. Wu and Q. S. Li, *Chem. Phys. Lett.*, 2006, **429**, 326–331.
37 X. An, H. Zhuo, W. Tian, Q. Li, W. Li and J. Cheng, *Mol. Phys.*, 2014, **112**, 2954–2962.
38 Q. S. Li and L. P. Cheng, *J. Phys. Chem. A*, 2003, **107**, 2882–2889.
39 M. N. Glukhovtsev, P. v. R. Schleyer and C. Maerker, *J. Phys. Chem.*, 1993, **97**, 8200–8206.
40 Y. C. Zhao, Z. G. Zhang, J. Y. Yuan, H. G. Xu and W. J. Zheng, *Chin. J. Chem. Phys.*, 2009, **22**, 655–662.
41 M. J. Frisch, G. W. Trucks, H. B. Schlegel, G. E. Scuseria, M. A. Robb, J. R. Cheeseman, G. Scalmani, V. Barone, B. Mennucci, G. A. Petersson, H. Nakatsuji, M. Caricato, X. Li, H. P. Hratchian, A. F. Izmaylov, J. Bloino, G. Zheng, J. L. Sonnenberg, M. Hada, M. Ehara, K. Toyota, R. Fukuda, J. Hasegawa, M. Ishida, T. Nakajima, Y. Honda, O. Kitao, H. Nakai, T. Vreven, J. A. Montgomery Jr, J. E. Peralta, F. Ogliaro, M. Bearpark, J. J. Heyd, E. Brothers, K. N. Kudin, V. N. Staroverov, R. Kobayashi, J. Normand, K. Raghavachari, A. Rendell, J. C. Burant, S. S. Iyengar, J. Tomasi, M. Cossi, J. M. M. N. Rega, M. Klene, J. E. Knox, J. B. Cross, V. Bakken, C. Adamo, J. Jaramillo, R. Gomperts, R. E. Stratmann, O. Yazyev, A. J. Austin, R. Cammi, C. Pomelli, J. W. Ochterski, R. L. Martin, K. Morokuma, V. G. Zakrzewski, G. A. Voth, P. Salvador, J. J. Dannenberg, S. Dapprich, A. D. Daniels, O. Farkas, J. B. Foresman, J. V. Ortiz, J. Cioslowski and D. J. Fox, *Gaussian 09, Revision A.02*, Gaussian, Inc., Wallingford, CT, 2009.
42 Y. Zhao and D. G. Truhlar, *Theor. Chem. Acc.*, 2008, **120**, 215–241.
43 R. Huenerbein, B. Schirmer, J. Moellmann and S. Grimme, *Phys. Chem. Chem. Phys.*, 2010, **12**, 6940–6948.
44 *CRC Handbook of Chemistry and Physics*, ed. W. M. Haynes, 95th edn, 2014–2015.
45 A. E. Reed, L. A. Curtiss and F. Weinhold, *Chem. Rev.*, 1988, **88**, 899–926.
46 M. N. Glukhovtsev, H. Jiao and P. v. R. Schleyer, *Inorg. Chem.*, 1996, **35**, 7124–7133.
47 M. T. Nguyen, *Coord. Chem. Rev.*, 2003, **244**, 93–113.
48 A. Korkin, A. Balkova, R. J. Bartlett, R. J. Boyd and P. R. Schleyer, *J. Phys. Chem.*, 1996, **100**, 5702.
49 L. Gagliardi and P. Pyykko, *J. Phys. Chem. A*, 2002, **106**, 4690–4694.
50 M. Lein, J. Frunzke, A. Timoshkin and G. Frenking, *Chem.–Eur. J.*, 2001, **7**, 4155–4163.
51 L. Jin and Y. Ding, *J. Phys. Chem. A*, 2009, **113**, 13645–13650.
52 S. Fau, K. J. Wilson and R. J. Bartlett, *J. Phys. Chem. A*, 2002, **106**, 4639–4644.
53 Y. Xu, Q. Wang, C. Shen, Q. Lin, P. Wang and M. Lu, *Nature*, 2017, **549**, 78–81.
54 C. Zhang, C. Yang, B. Hu, C. Yu, Z. Zheng and C. Sun, *Angew. Chem., Int. Ed.*, 2017, **56**, 1–4.